CHEMNANOMAT

CHEMISTRY OF NANOMATERIALS FOR ENERGY, BIOLOGY AND MORE

Accepted Article

Title: Dual-fluorescent nanoscale coordination polymers via a mixed-ligand synthetic strategy and their use for multichannel imaging

Authors: Fernando Novio, Fabiana Nador, Karolina Wnuk, Javier García-Pardo, Julia Lorenzo, Rubén Solorzano, and Daniel Ruiz-Molina

FULL PAPER

Dual-fluorescent nanoscale coordination polymers via a mixed-ligand synthetic strategy and their use for multichannel imaging

Dr. Fabiana Nador,*[a] Karolina Wnuk,[a] Dr. Javier García-Pardo,[a, b] Dr. Julia Lorenzo,[b] Rubén Solorzano,[a,c] Dr. Daniel Ruiz-Molina,[a] and Dr. Fernando Novio*[a,c]

Abstract: Two rationally-designed strategies for covalent bonding of fluorescent dyes in coordination polymer nanoparticles to achieve bifunctional fluorescent nanostructures have been developed. The first strategy was based on the synthesis of the coordination polymers structured as nanoparticles by coordination of Co^{II} ions to two different catechol ligands containing free functional chemical groups (dopamine and 3,4-dihydroxybenzaldehyde), and a bis-imidazol ligand (1,4-bis(imidazole-1-ylmethyl)benzene, bix). Subsequently, different dyes namely fluorescein isothiocyanate (FITC), 1-pyrenebutanoic acid hydrazide (PBH) or Alexa Fluor® 568 (A568) could be sequentially attached to the nanoparticles surface. The second strategy was focused on the pre-functionalization of catechol ligands with the corresponding dyes and afterward the coordination with the metal ions in presence of bix. In vitro studies demonstrated the internalization of the bifunctional nanoparticles and the persistence of the fluorescent properties after cell uptake without dye leaching.

Introduction

Nanoscale coordination Polymers (NCPs) have emerged as a promising new family of nanomaterials due to their low cost, facile production and multifunctionality.[1,2] The control of the self-assembly of metallic ions with polydentate bridging ligands under specific conditions has allowed to obtain a wide variety of nanoparticles with specific properties.[3,4] Due to their nature, NCPs exhibit the most interesting features of the organic polymeric nanoparticles (i.e. functionalization, encapsulation ability, hydrophobic or hydrophilic properties) and also of the inorganic metal-based particles (i.e. optical, magnetic or catalytic properties).[5] Therefore, NCPs have attracted broad interest on different application areas, from molecular electronics,[6-8]

[a] Dr. F. Nador, K. Wnuk, Dr. J. García-Pardo, R. Solorzano, Dr. D. Ruiz-Molina, Dr. F. Novio
Catalan Institute of Nanoscience and Nanotechnology (ICN2), CSIC and The Barcelona Institute of Science and Technology
Campus UAB, Bellaterra, 08193 Barcelona, Spain
fernando.novio@icn2.cat, fabiana.nador@icn2.cat

[b] Dr. J. Garcia-Pardo, Dra. J. Lorenzo
Institut de Biotecnologia i Biomedicina (IBB)
Departament de Bioquímica i de Biologia Molecular
Universitat Autònoma de Barcelona
Cerdanyola del Vallès, 08193 Barcelona, Spain

[c] Dr. F. Novio, R. Solorzano
Departament de Química
Universitat Autònoma de Barcelona
Cerdanyola del Vallès, Barcelona, Spain

sensors[9-12] or water remediation[13,14] to nanomedicine.[5,15,16]

In spite of these tremendous developments, the designed surface functionalization of NCPs still represents a challenge since it is a crucial step to tune their physicochemical properties or improve their colloidal stability and biocompatibility. We have reported previously the partial achievement of this goal through a stepwise synthesis and functionalization protocol that involves: I) first the synthesis of robust nanoparticles by incorporation of carboxyl groups and II) the subsequent functionalization of those carboxyl groups located on the surface through well-known coupling reactions.[16] Following this approach, enhanced colloidal stabilities and the incorporation of functional groups such as polyethylene glycol (PEG) or fluorescent dyes that enabled tracking of their cellular uptake, was achieved. This approach was also followed to covalently graft coordination polymers to amino-functionalized surfaces on the quest for novel hybrid interphases with potential technological applications.[17]

The opportunity of monitoring lower concentrations of dyes creates conditions for increasing the sensitivity and offers new possibilities in the use of nanoparticles as luminescent labels in biology. They take the advantages of noninvasive imaging of cells and tissues, the availability of plentiful fluorescence probes to label specific gene products or to visualize molecular interactions inside cells, high time resolution to trace movement of the nanomaterials inside cells, and high spatial resolution to analyze individual cells.[18] The interest to incorporate different fluorochromes and the quest for nanoparticles with diverse spectral emissions is nowadays a topic of intense research as they can make multi-channel fluorescence imaging feasible or allow for ratiometric sensing of local chemical environments within the cell.[19] Herein, on a step further to obtain dual-fluorescent nanoparticles, we report the use of mixed-ligand combinations to obtain NCPs with more than one surface functionalization group, as schematically depicted in Figure 1 (route 1). This approach involves the synthesis of the coordination polymer using two different functionalized catechol ligands containing free terminal amino (dopamine, **1**) or aldehyde chemical groups (3,4-dihydroxybenzaldehyde, **2**). Afterwards, those amine and aldehyde groups more accessible on the surface of the NCPs were subsequently reacted with fluorescein isothiocyanate (FITC) or 1-pyrenebutanoic acid hydrazide (PBH), respectively. Finally, and for comparison purposes, we have also developed an alternative strategy that consists first in the coupling of the fluorescent dyes (FITC and PBH) to the catechol ligands **1** and **2** respectively to get the corresponding pre-functionalized catechols (**L₁** and **L₂**) and subsequent coordination to also yield dual-fluorescent nanoparticles (see Route 2 in Figure 1). Experimental results will evidence how this second approach leads to the obtaining of highly dispersed and with a larger fraction of non-structured material, validating our initial approximation Route 1.
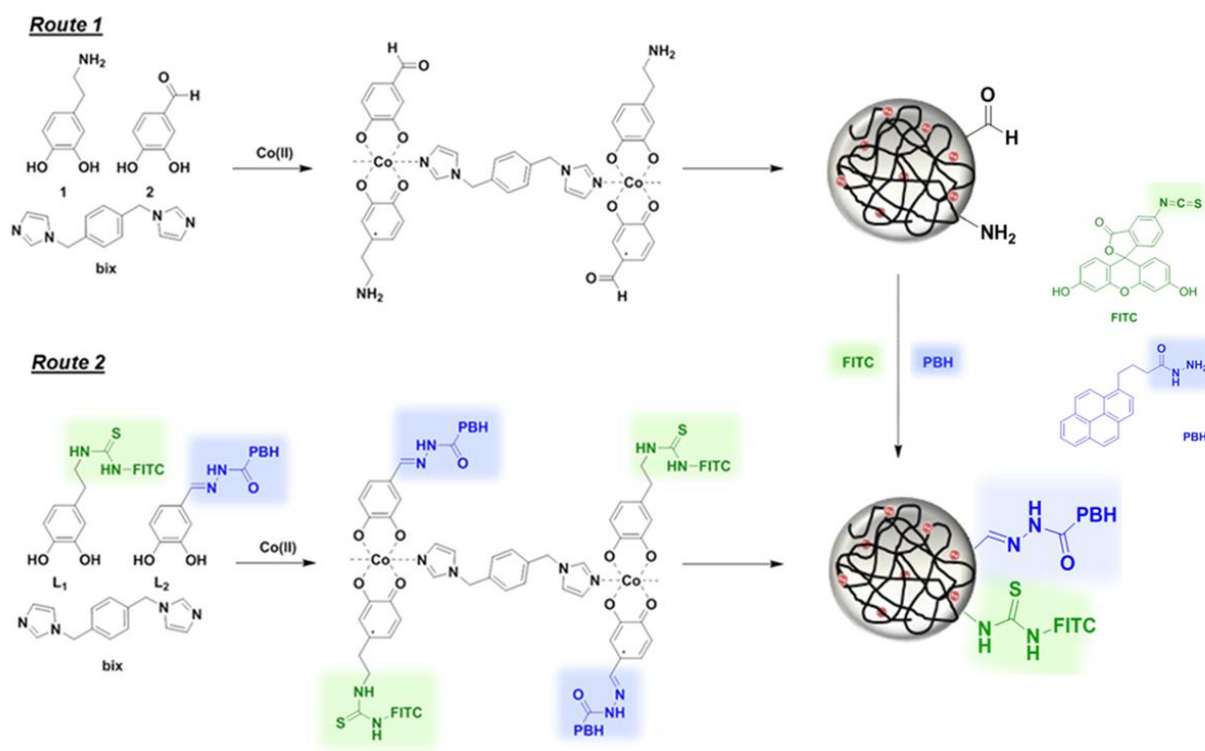
Figure 1. Schematic illustration describing two different routes to obtain dual-fluorescent NCPs. Route 1 shows the synthesis of the NCPs containing two different functional groups (amino and aldehyde) and the subsequent attachment of fluorescent dyes (FITC and PBH). Route 2 involves the preparation of NCPs from pre-functionalized catechol ligands with the corresponding fluorescent dyes FITC (L_1) and PBH (L_2).

Results and Discussion

Route 1: surface functionalization

Prior to any dual surface functionalization, NCPs containing only one of the cathecol ligands were obtained and its reactivity in front of the giving dye checked.

Monofunctional nanoparticles. Adapting an experimental procedure previously published in our group,[16] the monofunctional coordination polymer particles bearing only dopamine (dopa) (NCP_1) or 3,4-dihydroxybenzaldehyde (DHBA) (NCP_2) as catechol ligands were first obtained as model nanoparticles by reaction of a cobalt salt with the corresponding ligand and bix as a polymeric linker with a 1:2:1 ratio. The choose of cobalt as a metal node has been shown to offer better reproducibility while minimizing quenching effects as by comparison with other metal ions such as iron while exhibiting low cytotoxicity. Moreover, related cobalt complexes have been used for paramagnetic chemical exchange saturation transfer (paraCEST) MRI as published very recently.[20]

The reaction leads in both cases to the formation of a coordination polymer that precipitates as nanoparticles due to their low solubility in the reaction medium. The resulting NCPs were subsequently collected by centrifugation, washed with water and ethanol, and then dried (for detailed preparation procedure see Experimental Section). The formation of spherical nanoparticles with average diameters of 37 ± 7 nm and 150 ± 50 nm for NCP_1 and NCP_2 respectively, was observed by scanning electron microscopy images (SEM) (see Supporting Information, Figure S1). X-ray diffraction experiments confirmed the amorphous character of these materials (see Supporting Information, Figure S2). Infrared Spectroscopy (FT-IR) corroborates the presence of the bands of the corresponding ligands (see Supporting Information, Figure S3). Combined chemical analysis of the nanoparticles by elemental analysis (EA), inductive coupled plasma (ICP-MS), NMR and HPLC indicate a chemical composition that fit with a formula $[Co(dopa)_{0.5}(bix)(AcO)_{0.5}(H_2O)_3]$ and $[Co(DHBA)(bix)(AcO)_{0.5}(H_2O)_2]$ for NCP_1 and NCP_2, respectively (see Supporting Information S1). The catechol ligand content is around 17% w/w for NCP_1 and 28% for NCP_2. The final composition differs from the expected from the initial reactants ratio most likely due to the different affinity of Co(II) for imidazole or catechol ligands, and the formation of the nanoparticles out of equilibrium conditions (fast precipitation process) induced by their low solubility on the reaction media.

In a subsequent step, the nanoparticles were functionalized with the dyes (for more details see Experimental Section). NCP_1 nanoparticles were functionalized with FITC (NCP_1-FITC) by addition of the fluorescein isothiocyanate to a dispersion of the NCP_1 nanoparticles in acetone containing a K_2CO_3 buffer (pH~9) and stirring at 4 °C under nitrogen atmosphere for 8 hours. Alternatively, an ethanolic dispersion of NCP_2 nanoparticles was reacted with PBH in the presence of acetic acid for 6 h under

reflux to yield nanoparticles of **NCP₂-PBH.** In both cases, the resulting solid material was centrifuged, washed until no fluorescence was detected in the solution, and dried under vacuum. SEM images revealed no significant differences in neither size nor morphology with respect to the original non-functionalized nanoparticles (see Supporting Information S2.a). UV-Vis measurements confirmed the attachment of the dyes upon particle digestion in a MeOH/HCl(conc.) mixture and measurement of the final solution. Moreover, quantification of the dyes loading was done upon comparison of the corresponding Uv-Vis spectra with a standard calibration curve (absorbance vs. concentration) of the pure dye in acid medium. Values of 7 % w/w of **FITC** and 6% w/w of **PBH** per mg of nanoparticle were obtained (see Supporting Information, S2.b).

Bifunctional nanoparticles. Nanoparticles containing a mixture of both catechol ligands (dopamine/3,4-dihydroxybenzaldehyde) were also synthesized (**NCP₃**) using similar experimental conditions to those previously described but now using an initial 50:50 mixture of both catechol ligands (for more experimental details see Experimental Section and for complete characterization data see the Supporting Information, S3). The reaction afforded nanoparticles with an average diameter of 60 ± 30 nm. FT-IR confirmed the presence of dopamine, 3,4-dihydroxybenzaldehyde, and bix ligand based principally on the presence of the υN-H and υC-NH stretching bands of the amine group from dopamine at 3350 and 1490 cm^{-1} respectively, the υC=O stretching mode of aldehyde group from 3,4-dihydroxybenzaldehyde centered at 1658 cm^{-1}, the υC-O stretching mode of the catecholate coordinated moieties between 1250-1334 cm^{-1}, and the corresponding typical signals of bix at 3139, 1234, and 1108 cm^{-1}. Combined analysis by ^{1}H-NMR, EA and ICP-MS analysis resulted in a chemical composition for **NCP₃** of [Co(dopa)$_{0.5}$(DHBA)(bix)(AcO)$_{0.5}$(H₂O)]. The nanoparticles contain a 38% w/w of catechol ligands (13.6%w/w dopa, 24.5%w/w DHBA) with a relative 1:2 ratio of dopamine:dihydroxybenzaldehyde, value in good agreement with the results obtained by HPLC after dissolving the **NCP₃** in acidic media 0.42:0.89:1 (dopa:DHBA:bix). These values correspond to a 8.9% w/w and a 26.6% w/w of dopamine and 3,4-dihydroxybenzaldehyde, respectively.
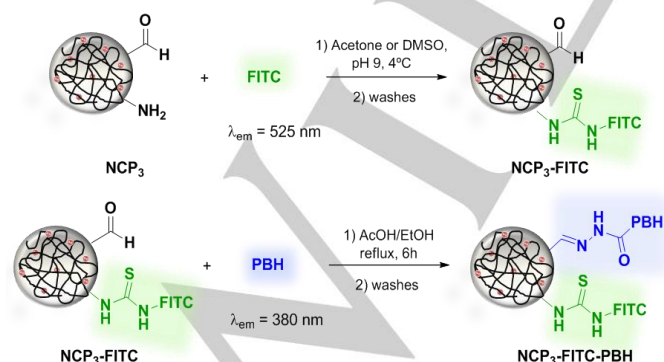
Once synthesized and characterized, **NCP₃** nanoparticles were functionalized with **FITC** following the experimental conditions previously optimized for **NCP₁-FITC** (see Figure 2a and Experimental section). The resulting **NCP₃-FITC** nanoparticles are washed until free **FITC** is completely removed, and afterwards dried under vacuum. SEM images revealed no significant modification of the size (64 ± 28 nm) nor the morphology with respect to the original **NCP₃** nanoparticles (see Figures 3a). Moreover, spectroscopic measurements shown in Figure 3b reveal bands associated to both, **NCP₃** and **FITC** systems, confirming the attachment of the fluorescent dye. **NCP₃-FITC** nanoparticles were subsequently dispersed in ethanol and reacted with **PBH** using the same experimental conditions than those previously optimized for monofunctional **NCP₂-PBH** nanoparticles (see Figure 2b). The resulting nanoparticles **NCP₃-FITC-PBH** were washed to remove free dye and dried under vacuum overnight and fully characterized. SEM images revealed again no significant modification of the size (62 ± 34 nm) or morphology (see Figure 3c). Spectroscopic measurements corroborated the attachment of the two fluorescent dyes (see Figure 3d). Quantification of dyes in **NCP₃-FITC-PBH** was done by HPLC (see the Supporting Information, S4), showing the presence of around 2.6 % w/w of **FITC** and 2.8 % w/w of **PBH** per mg of nanoparticle. According to the presence of both dyes, fluorescent optical micrographs of **NCP₃-FITC-PBH** nanoparticles in solid state revealed green and blue fluorescence emission characteristic of the attached dyes on the nanoparticles (see Figures 3e-f).
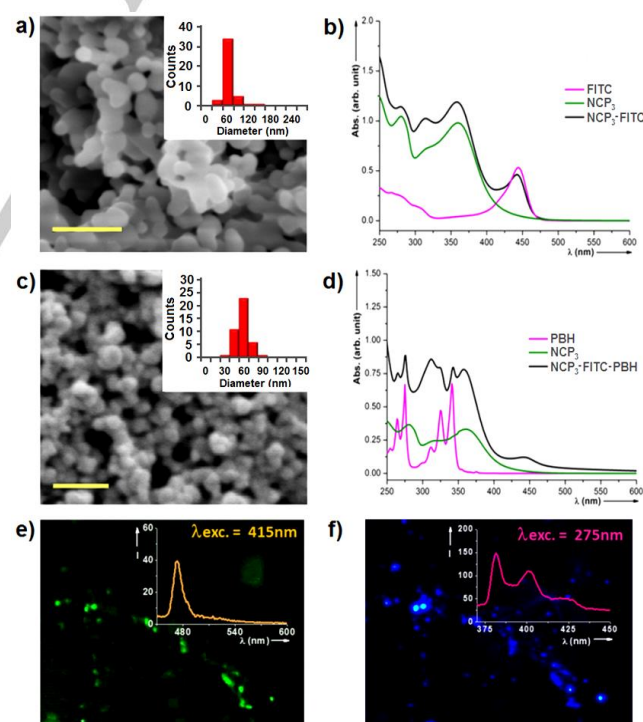
Figure 3. SEM images of **NCP₃-FITC** (a) and **NCP₃-FITC-PBH** (c) nanoparticles; UV-Vis spectra of **NCP₃-FITC** (b) and **NCP₃-FITC-PBH (d)** e-f) Fluorescence microscope images of **NCP₃-FITC-PBH**. Scale bars for SEM images are 250 nm. The inset depicts the fluorescence emission spectra of NCPs collected at $\lambda_{exc.}$ = 415 nm (FITC) or $\lambda_{exc.}$ = 275 nm (PBH).

Figure 2. (Top) Schematic illustration showing the coupling reaction conditions for the formation of **NCP₃-FITC** through a thio-urea bond, and (bottom) the coupling reaction conditions for the formation of **NCP₃-FITC-PBH** through an acyl hydrazone bond.

Route 2: ligand functionalization and synthesis of the nanoparticles

Synthesis of ligands L₁ and L₂. Synthesis of pre-functionalized ligands **L₁** and **L₂** is shown in Figure 4. In the case of dopamine the reaction takes place between its primary amine and the isothiocyanate group of the **FITC** to generate the new ligand **L₁** through the formation of a urea bond type. Ligand **L₂** was obtained by nucleophilic addition of hydrazine group from **PBH** to the carbonyl group of the 3,4-dihydroxybenzaldehyde, providing an hydrazone bond type. Both ligands were fully characterized by UV-Vis, FT-IR and NMR. In the case of **L₂** two conformational isomers coming from the rotation around the amide bond were found.[22] In general, UV-Vis absorption spectra of ligands **L₁** and **L₂** showed no modification with respect to those of the free dyes (see supporting Information S5). Only a slight red-shift of **L₁** compared to the free **FITC** dye was observed (for more details see Experimental Section).

Synthesis of monofunctional nanoparticles. As previously done for route 1, synthesis of the monofunctional nanoparticles was originally done to optimize reaction conditions. Thus, monofunctionalized NCPs were obtained upon reaction of an aqueous solution of Co(CH₃COO)₂·4H₂O with an ethanolic solution containing only one of the fluorescent ligands (**L₁** or **L₂**) and bix in a ratio 1:2:1. The resulting precipitates, named from now on as **NCP-L₁** and **NCP-L₂**, were washed, filtered, dried under vacuum and fully characterized by SEM, NMR, FT-IR and UV-Vis techniques (see Supporting Information, S6). SEM images revealed the formation of mixtures of round-shaped nanoparticles with very high polydispersity of sizes (ranging from a few nanometers to microns) combined with amorphous material. ¹H NMR and FT-IR of the **NCP-L₁** and **NCP-L₂** nanoparticles indicated the presence of both ligands bix/**L₁** and bix/**L₂**, respectively. Moreover, the concentration of dye ligands in both families of nanoparticles was calculated by absorbance measurements after degradation of the nanoparticles by addition of HCl (conc.). The results obtained were 37 % w/w of **L₁** for **NCP-L₁** and 70 % w/w of **L₂** for **NCP-L₂** (per mg of nanoparticle). These results differ from theoretical results according to the initial 1:2:1 (Co:L:bix) ratio (78 % w/w of **L₁** for **NCP-L₁** and 74 % w/w of **L₂** for **NCP-L₂**).

Synthesis of bifunctional nanoparticles. Nanoparticles **NCP-L₁-L₂** were synthesized using an equimolar mixture of **L₁**, **L₂** and bix dissolved in ethanol. This solution was mixed with an aqueous solution of Co(CH₃COO)₂·4H₂O, obtaining a dark brown precipitate, which was chemically and morphologically characterized. SEM images revealed the formation of mixtures of round-shaped nanoparticles combined with non-structured material. Moreover a very high polydispersity of sizes with two main (but not exclusively) populations of particles centered ~150 nm and >1μm (see Figure 5a) were obtained. Absorption and fluorescence emission spectra for the bifunctional nanoparticles showed the corresponding bands attributed to **L₁** and **L₂** (see Figures 5b-c). Moreover, the amount of **L₁** and **L₂** calculated by absorbance measurements after degradation of the nanoparticles in acidic media resulted in 30 % w/w for each dye per mg of nanoparticles. Again the obtained values are lower

than theoretical ones corresponding (43 % w/w of **L₁** and 34 % of **L₂** for a ratio Co:**L₁**:**L₂**:bix equal to 1:1:1:1). The enormous variability in size has been attributed to the presence of rather bulky groups in the ligands, and the supramolecular interactions and self-assembly process induced by FITC and PBH[21, 23] that can interfere in the homogenization of the resulting nanoparticles.
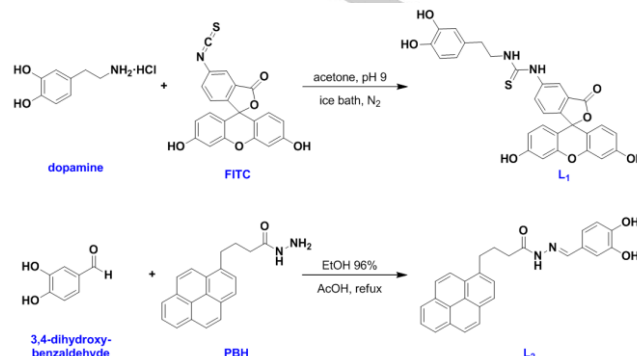
Figure 4. a) Synthesis of **L₁** ligand by coupling reaction between dopamine hydrochloride and fluorescein isothiocyanate (FITC); b) Synthesis of **L₂** ligand by condensation reaction between 3,4-dihydroxybenzaldehyde and 1-pyrenebutyric hydrazide (PBH).

Figure 5. a) SEM images of **NCP-L₁-L₂** (scale bars are 1μm), b) UV-Vis of digested **NCP-L₁-L₂** nanoparticles (1 mg) in a MeOH/HCl mixture (2.5 mL) and c) fluorescence emission (MeOH) spectra of **NCP-L₁-L₂** measured at λexc = 275 nm and 415 nm in MeOH and plotted in the same graphic.

*Synthesis of **NCP₃** nanoparticles doped with **L₁** and **L₂**.* A final attempt to obtain double-functionalised nanoparticles was done by combining route 1 and route 2 within the same experiment. For this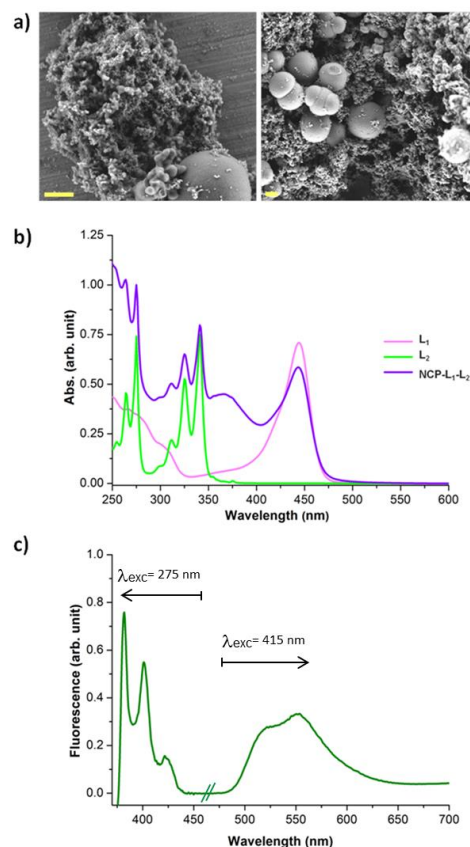, **NCP₃** nanoparticles were doped during its synthesis with small percentages of ligands **L₁** and **L₂**. The optimal conditions were obtained combining dye-functionalized (2.5 % of **L₁** and **L₂**) and non-funtionalized catechol ligands (97.5% of dopa and DHBA ratio 50:50). Relatively monodisperse nanoparticles with sizes below 150 nm were obtained (see Supporting Information S7 for complete characterization). Percentages above 2.5% of dye-functionalized ligands results in increased polydipersitivity. Although UV-Vis spectrum do not allow the quantification of both dyes due to signal overlapping with catechol ligands, HPLC analysis of the NCPs decomposed in acidic media indicates the presence of 0.9 % and 1.2 % w/w of **L₁** and **L₂** per mg of nanoparticles, values close to the initial ratios used. In any case, the result obtained does not improve those obtained with our route 1, i.e. **NCP₃-FITC-PBH**.

In basis of the obtaining results, we conclude that the one-pot synthesis of the bifunctional systems starting from the pre-functionalized ligands **L₁** and **L₂** offer more difficulties to obtain homogeneous nanoparticles in a reproducible manner. The homogenization in size can be achieved only when the bifunctional nanoparticles are synthesized using an small amount of pre-functionalized ligands (less than 2.5%), but this limitation imply a reduction of the dyes content in the final material. As the best results concerning dye content, sample homogenizity and reproducibility were obtained for the two-step synthesis the studies of toxicity and cellular uptake were performed using **NCP₃-FITC-PBH** nanoparticles.

Toxicity and Cellular uptake

Emissive **NCP₃-FITC-PBH** and non-emissive **NCP₃** nanoparticles (used as a blank) were dispersed in DMSO (0.1mg/mL) under sonication and then an aliquot of 0.2 mL was taken and further diluted in 1.8 mL of PBS-albumin solution (0.5 mM) mimicking biological conditions. Zeta-potential measurements of **NCP₃-FITC-PBH** and **NCP₃** in PBS-BSA solution offered values of -14.0 ± 0.8 mV and -18.7 ± 1.9 mV respectively (see Supporting Information, Section S8). Under these conditions, average diameters obtained by DLS (175 ± 15 nm for **NCP₃**; 210 ± 10 nm for **NCP₃-FITC-PBH**) were slightly larger than those found by SEM (60 ± 30 nm). Such divergence might be attributed to the albumin coating and/or to the tendency to form small nanoparticle clusters in presence of BSA. In any case, the resulting solutions were stable for several hours, confirming that our nanoparticles are suitable for cytotoxicity and cellular uptake experiments.

The effects of the **NCP₃-FITC-PBH** nanoparticles on the cell viability of HeLa cells was examined after 24h of exposure, using a resazurin-based assay. As shown in Supporting information (see the Supporting Information, S9-Figure S26), concentrations up to 100 μg/ml of nanoparticles did not affect cell viability significantly (>80% cell viability in all the cases). This finding is in agreement with previous reports for other related systems,[15,16] and demonstrates that the chemical composition of the present nanoparticles (with a relatively low percentage of metal ions) does not contribute to toxicity. Next, we evaluated the cellular uptake of **NCP₃-FITC-PBH** nanoparticles in HeLa cells by using confocal laser scanning microscopy (CLSM). In an initial experiment we clearly observed the emission of the **PBH** in the 380-420 nm range inside cells upon excitation at 410 nm. Similarly, **FITC** fluorescence was detected in the cytoplasm and nuclei of HeLA cells co-localized with the **PBH** emission (see Supporting Information, S9-Figure S27). Unfortunately, a partial overlap between the blue emission from PBH and the emission of nuclear stains (such Hoechst®) was observed. With the aim to develop a novel generation of bifunctional nanoparticles that do not overlap with nuclear stains, a new fluorescent dye (Alexa Fluor® 568) which emits in the red region and contains the same reactive hydrazide group as **PBH**, was used in combination with **FITC** to functionalize the **NCP₃**
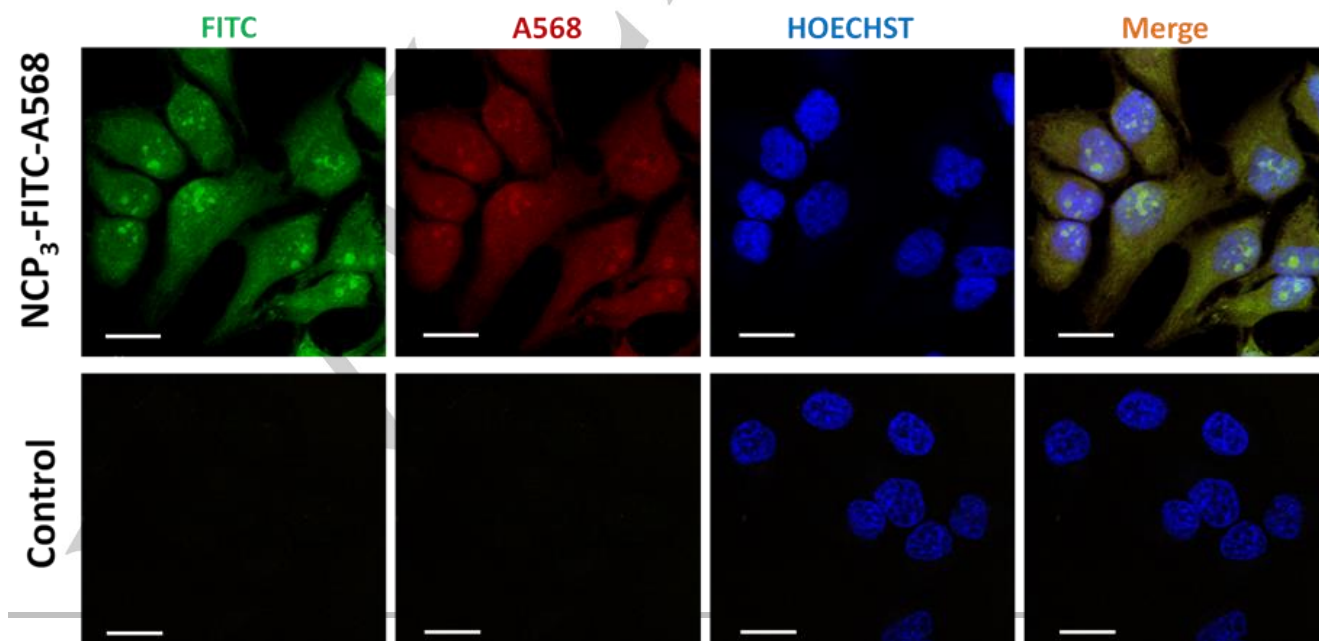
Figure 6. Cellular uptake of nanoparticles by HeLa cells. Confocal Laser Scanning Microscopy (CLSM) *in vivo* images of HeLa cells treated for 2 h with **NCP₃-FITC-A568** and non-functionalized **NCP₃** (control). The maximum projections of images of individual channels show the localization of **FITC** (in green), **A568** (in red), the nuclear stain (Hoechst, in blue) and the colocalization of all channels (merge). The excitation wavelength for FITC, A568 and Hoechst stain were λ_{exc}=561 nm, λ_{exc}=488 nm and λ_{exc}=405 nm, respectively. Scale bars are 20 μm.

particles. Thus, using similar reaction conditions to those used for **NCP₃-FITC-PBH**, Alexa Fluor® 568 (**A568**) was included instead **PBH** (see Experimental Section). The characterization of this new system **NCP₃-FITC-A568** is detailed in Supporting Information S10. The resulting nanoparticles exhibit a relatively good colloidal stability in PBS-BSA, with Zeta potential (-10.0 ± 1.2 mV) and DLS (196 ± 51 nm). Moreover, the cytotoxic effect of the **NCP₃-FITC-A568** nanoparticles on the cell viability of HeLa cells examined after 24h of exposure showed the same pattern that **NCP₃-FITC-PBH** with low toxicity (>80% cell viability for concentrations up to 100 µg/ml of nanoparticles).

For testing the cellular uptake, 0.1 mg/mL of **NCP₃-FITC-A568** and non-functionalized **NCP₃** nanoparticles (as control) were put in contact with HeLa cells for 2 h at 37 ºC. Before *in vivo* imaging, cells were washed gently with fresh medium and the cell nuclei were then stained with Hoechst dye for 10 min. Fluorescence imaging obtained by confocal fluorescence microscope confirmed the intracellular uptake of the dual fluorescent probes (see Figure 6). A quantitative colocalization analysis revealed that approximately 90% of all **FITC** fluorescent emission in the region of interest was overlapping with the A568 emission (with a Pearson's correlation coefficient = 0.75). This result suggested that bifunctional nanoparticles could be internalized by HeLa cells and both dyes remained attached to the nanoparticles after 2 hours uptake. In contrast, no fluorescence from the **NCP₃** nanoparticles was detected in control cells (see Figure 6). It is noteworthy to mention that an important part of the particles are found in the nucleolus of the cells, while only a small fraction was found in the cytoplasm (see the Supporting Information, S11). Nucleoli are large structure located inside the nucleus of eukaryotic cells and contain most of the nuclear RNA. These observations have been already published for other authors, who showed that some styrylpyridine dyes (like presumably **A568**) have good affinity for RNA.[24] Previous published works demonstrated that larger polymeric materials with a size >100 nm, such chitosan nanoparticles, with higher plasticity, are capable of localizing in the nucleus.[25, 26] Thus, it is not unreasonable to think that large organic or inorganic structures as **NCP₃-FITC-A568** nanoparticles can entry into the nucleus without important disruption. Finally, to confirm the internalization of **NCP₃-FITC-A568** nanoparticles by HeLa cells, the **FITC** and **A568** fluorescence was measured from the cellular fraction using a spectrofluorimeter. To perform the experiments, HeLa cells were incubated with different nanoparticle concentrations (0, 50 and 100 µg/mL) for 2 h, and then lysed in PBS containing 1 % sodium dodecyl sulfate (SDS). As expected, results showed a dose-dependent increase in the fluorescence levels for **FITC** and **A568** in the intracellular fraction of HeLa cells treated with the **NCP₃-FITC-A568** nanoparticles (see Supporting Information, S12). This data also confirm the fluorescent stability of such dyes after cellular internalization of the nanoparticles.

Conclusions

We have reported the synthesis of dual-fluorescent nanoscale coordination polymers via a mixed-ligand synthetic strategy. For this, a two-step protocol is followed: I) first the synthesis of robust nanoparticles by incorporation of ligands bearing amino and carbonyl groups and II) the subsequent functionalization with different dyes (FITC and PBH) of those amino and carbonyl groups located on the surface through well-known coupling reactions. This approach (route 1) allows for the synthesis of nanoparticles with a defined control over their emission properties and morphology, bearing dye loadings close to 3% w/w. Alternatively, the pre-functionalization of the ligands with the dyes and posterior formation of the nanoparticles (route 2) offers higher payloads but with a detrimental control of the morphology and dimensions. Monodispersed nanoparticles, though not so well defined, are obtained when the synthesis of the NCPs is performed using a low quantity (2.5%) of pre-functionalized ligands what reduced notably the amount of fluorescent dyes in comparison with those obtained by route 1. These results validate route 1 as a successful approach for the synthesis of multifunctional NCPs.

Finally, and as proof-of-concept to demonstrate the new venues that these multifunctional nanoparticles may open in bioimaging, the cytotoxicity and cell internalization of **NCP₃-FITC-PBH** nanoparticles was studied. None of the nanoparticles tested exhibit side cytotoxic effects even the presence of the metal ion, most likely due to its low concentration, Concerning cell internalization assays, the emission of the **PBH** in the 380-420 nm range overlapped with the blue emission from the Hoechst dye staining nucleus so it was replaced by the Alexa Fluor® 568 dye, which emits in the red region. Upon exposition of the **NCP₃-FITC-A568** nanoparticles to HeLa cells, internalization was followed at two different wavelengths making multi-channel biological fluorescence imaging feasible.

This proposed methodology allows functionalize NCPs with a wide variety of fluorescent dyes. The combination of dyes can afford combined fluorescent probes available with a range of emission colours spreading through visible to near-infrared wavelengths. Simultaneous use of different dyes with spectrally distinct emissions makes multi-channel biological fluorescence imaging feasible. Such dual-wavelength emission properties could also serve as the basis for ratio metric sensing local chemical environment of the cells when sensitive dyes are used. Additionally, the capability of surface functionalization of these nanoparticles by specific molecules, one could develop nanoparticles that recognize the biological targets or monitor the transformation of the tumors by simultaneously non-invasive fluorescence imaging.

Experimental Section

Materials

All reactants and reagents were purchased from Sigma–Aldrich and used as received. Solvents were purchased from Scharlab and used as received. Cell culture media and supplements were obtained from Life Technologies. Nuclear magnetic resonance (NMR) spectra were recorded on a Bruker ARX-400 and ARX-250 spectrophotometer using acetone-d_6, methanol-d_4, dimethyl sulfoxide-d_6 or a mixture of MeOD/DCl in order to register NCPs. FT-IR spectra were collected on a Tensor 27 FT-IR Spectrometer (Bruker) in the range of 400-4000 cm^{-1} using KBr pellets. UV-Vis spectra were obtained on a Cary 4000 spectrophotometer (Agilent) using quartz cuvettes. Emission spectra were measured by means of a custom-made spectrofluorimeter, in which a continuous wave (CW) He–Ne Research Electro Optics (REO) laser (λexc=594 nm) was used as an excitation source and the emitted photons were detected in an Andor ICCD camera coupled to a spectrograph. SEM images were obtained by a scanning electron microscope (FEI Quanta 650 FEG and FEI Magellan 400L XHR) at acceleration voltages of 2–5 kV. Aluminium was used as support. Optical and fluorescence images were registered by Zeiss Axio Observer Z-1 inverted optical/fluorescence microscope with motorized XY stage, Hg lamp excitation source, AxioCam HRc digital camera and standard filters. Size distribution and surface charge of the nanoparticles were measured by DLS, using the Zetasizer Nano 3600 instrument (Malvern Instruments, UK), whose size range limit is 0.6 nm to 6 μm (5 nm to 10 μm for zeta-potential). *In vivo* fluorescence imaging was performed in a Leica TCS SP5 confocal fluorescence microscope. FITC and A568 Fluorescence were measured in a Jasco FP-8200 spectrofluorometer.

Synthesis of NCP₁, NCP₂ and NCP₃

*Preparation of **NCP₁**:* a mixture of dopamine (0.5 mmol, 94.5 mg) and bix (0.25 mmol, 59.5 mg) was dissolved in 15 mL of EtOH. Under magnetic stirring (700 rpm) the addition of an aqueous solution of $Co(CH_3COO)_2 \cdot 4H_2O$ (0.25 mmol, 62.3 mg) led to a color change from colourless to black. A fine precipitate rapidly formed and after stirring at room temperature for 2 hours, the precipitate was centrifuged (8000 rpm) and washed with water and EtOH three times (15 mL). The solvent was removed and the solid dried under vacuum and characterized.

*Preparation of **NCP₂**:* a mixture of 3,4-dihydroxybenzaldehyde (0.5 mmol, 69 mg) and bix (0.25 mmol, 59.5 mg) was dissolved in MeOH or acetone (10 mL). In addition, $Co(CH_3COO)_2 \cdot 4H_2O$ (0.25 mmol, 62.3 mg) was placed in a vial and dissolved in 4 mL of water. The mixture of ligands was slowly added to the aqueous solution forming a new phase. A green solid started to form in the interphase, precipitating after few hours. The reaction was left for 48 h without stirring and finally the precipitate was centrifuged (8000 rpm) and washed with water and MeOH three times (15 mL).

*Preparation of **NCP₃**:* A mixture of dopamine (0.25 mmol, 47.3 mg), 3,4-dihydroxybenzaldehyde (0.25 mmol, 34.5 mg) and bix (0.25 mmol, 59 mg) was dissolved in 15 mL of EtOH. Under magnetic stirring (700 rpm) the addition of an aqueous solution of $Co(CH_3COO)_2 \cdot 4H_2O$ (0.25 mmol, 62.3 mg) led to a colour change from colourless to black. A fine precipitate rapidly formed and after stirring at room temperature for 2 hours, the precipitate was centrifuged (8000 rpm) and washed with water and EtOH three times (15 mL). The solvent was removed and the solid dried under vacuum and fully characterized.

Synthesis of NCP₁-FITC and NCP₂-PBH

*Preparation of **NCP₁-FITC**:* NCP₁ (30 mg) in Na₂CO₃ buffer (0.1M, pH~9, 2 mL) was mixed with a solution of FITC (0.013 mmol, 5 mg) in acetone (5 mL) or DMSO (2 mL) and stirred at 4 °C under nitrogen atmosphere. After 8 h the precipitate was centrifuged (8000 rpm) and washed with water and MeOH three times (15 mL) until no free dye was detected in the supernatant solution. Finally, the solvent was removed and the solid dried under vacuum and characterized.

*Preparation of **NCP₂-PBH**:* PBH (0.01 mmol, 3 mg) and acetic acid (10 μL) were added to a stirring dispersion of **NCP₂** (8 mg) in EtOH (6 mL).

The mixture was stirred under reflux for 6 hours. The resulting particles were purified by centrifugation, and then washed with water, acetonitrile and MeOH three times (15 mL) until no free dye was detected in the supernatant solution. The precipitate was dried under vacuum overnight and fully characterized.

Synthesis of NCP₃-FITC-PBH (Route 1)

Sequential attachment of FITC and PBH fluorescent dyes: NCP₃ (30 mg) in K₂CO₃ buffer (0.1M, pH~9, 2 mL) was mixed with a solution of **FITC** (0.013 mmol, 5 mg) in acetone (5 mL) or DMSO (2 mL) and stirred at 4 °C under nitrogen atmosphere. After 8 h, the precipitate was centrifuged (8000 rpm) and washed with water and MeOH until no free dye was detected in the supernatant solution. The solvent was removed and the solid (**NCP₃-FITC**) was dried under vacuum and characterized. In a second step, **PBH** (0.017 mmol, 5 mg) and acetic acid (10 mL) were added to a stirring dispersion of **NCP₃-FITC** (30 mg) in 6 mL of EtOH. The mixture was stirred under reflux for 6 h. The resulting particles were purified by centrifugation, and then washed with water, acetonitrile and MeOH (3 mL per wash) until no free dye was detected in the supernatant solution. The precipitate (**NCP₃-FITC-PBH**) was dried under vacuum overnight and fully characterized.

Synthesis of ligand L₁

A solution of dopamine hydrochloride (**1**, 0.1 mmol, 18.9 mg) in K₂CO₃ buffer (0.1 M, pH~9, 2 mL) was mixed with a solution of FITC (0.1 mmol, 38.9 mg) in 5 mL of acetone (or 2 mL of DMSO) and stirred in an ice bath under nitrogen atmosphere. After 8 h the acetone was evaporated under vacuum, while in the case of DMSO it was removed by washing in a water/AcOEt mixture. The crude was purified by chromatographic column obtaining a yield of **L₁** around 50%. ^{1}H NMR (250 MHz): δ = 2.85 (t), 3.82 (t), 6.59-6.63 (m), 6.70-6.76 (m), 6.81-6.88 (m), 7.16 (d), 7.66 (dd), 8.15 (s). ^{13}C NMR (400 MHz): δ = 34.8, 46.6, 84.1, 103.3, 110.0, 110.7, 110.8, 113.6, 113.7, 116.6, 117.0, 120.4, 130.0, 130.1, 130.9, 142.3, 144.7, 146.2, 148.2, 153.0, 160.5, 169.6, 181.3.

Synthesis of ligand L₂

A mixture of PBH (0.06 mmol, 18 mg), 3,4-dihydroxybenzaldehyde (**2**, 0.05 mmol, 7 mg) and acetic acid (10 μL) in EtOH 96 % (6 mL) was stirred and heated under reflux for 6 hours. The solvent was then evaporated and the residue was washed with water and centrifuged. ^{1}H NMR (360 MHz, CD₃COCD₃) δ 10.10 (s), 8.51 (d'), 8.27 – 8.12 (m), 8.08 (d), 8.07 – 7.93 (m), 7.92 (s), 7.32 (d), 6.96 (dd), 6.85 (d), 3.55 – 3.34 (m), 2.91 (t), 2.23 (quint). ^{13}C NMR (91 MHz, CD₃COCD₃) δ 174.79, 148.37, 146.30, 143.85, 137.80, 132.31, 131.87, 130.75, 128.41, 128.39, 128.10, 127.80, 127.42, 127.38, 126.83, 126.80, 125.82, 125.78, 124.57, 124.48, 121.11, 116.13, 113.63, 33.79, 33.03, 28.28.

Synthesis of NCP-L₁, NCP-L₂ and NCP-L₁-L₂ (Route 2)

*Preparation of **NCP-L₁**:* a mixture of **L₁** (0.018 mmol, 10 mg) and bix (0.0092 mmol, 2.2 mg) was dissolved in 5 mL of EtOH. Under magnetic stirring (700 rpm) the addition of an aqueous solution of $Co(CH_3COO)_2 \cdot 4H_2O$ (0.0092 mmol, 2.3 mg in 0.5 mL of water) led to a change in colour from light orange to dark orange. A fine precipitate was rapidly formed and after stirring at room temperature for 2 hours, the precipitate was centrifuged (10000 rpm) and washed with water and EtOH three times (15 mL). The solvent was removed and the solid dried under vacuum and characterized.

*Preparation of **NCP-L₂**:* a mixture of **L₂** (30 mg, 0.071 mmol) and bix (0.036 mmol, 8.6 mg) was dissolved in 3 mL of MeOH. $Co(CH_3COO)_2 \cdot 4H_2O$ (0.036 mmol, 9 mg) and placed in a vial and dissolved in 0.5 mL of water. The mixture of ligands was slowly added to the aqueous solution forming a new phase. After 3-4 hours, a green solid started to form in the interphase and then precipitated on the bottom of the vial. The reaction was left for 48 h without stirring and finally the precipitate was centrifuged (8000 rpm) and washed with water and

MeOH three times (15 mL). The solvent was removed and the solid dried under vacuum and fully characterized.

*Preparation of the double fluorescence **NCP-L₁-L₂** nanosystem:* A mixture of **L₁** (0.02 mmol, 10.9 mg), **L₂** (0.02 mmol, 8.5 mg) and bix (0.02 mmol, 4.8 mg) was dissolved in 6 mL of EtOH. Under magnetic stirring (700 rpm) the addition of an aqueous solution of $Co(CH_3COO)_2·4H_2O$ (0.02 mmol, 5 mg) led to a colour change from light brown to dark brown. A fine precipitate rapidly formed and after stirring at room temperature for 2 hours, the precipitate was centrifuged (10000 rpm) and washed with water and EtOH three times (15 mL). The solvent was removed and the solid dried under vacuum and characterized.

Synthesis of NCP₃-L₁-L₂(2.5%) by mixing catechols and pre-functionalized ligands L₁ and L₂

*Preparation of **NCP₃-L₁-L₂(2.5%)**:* a mixture of dopamine (0.49 mmol, 92.6 mg), 3,4-dihydroxybenzaldehyde (0.49 mmol, 67.6 mg), **L₁** (0.01 mmol, 5.4 mg), **L₂** (0.01 mmol, 4.2 mg) and bix (0.5 mmol, 119 mg) was dissolved in 15 mL of EtOH. Under magnetic stirring (700 rpm) the addition of an aqueous solution of $Co(CH_3COO)_2·4H_2O$ (0.5 mmol, 124.5 mg) led to a colour change from colourless to dark blue. A fine precipitate rapidly formed and after stirring at room temperature for 2 hours, the precipitate was centrifuged (8000 rpm) and washed with water and EtOH three times (15 mL). The solvent was removed and the solid dried under vacuum and fully characterized.

Synthesis of the double fluorescent nanoparticles (NCP₃-FITC-A568) by attaching FITC and A568 dyes on NCP₃ surface

*Sequential attachment of **FITC** and **A568** fluorescent dyes:* **NCP₃** (30 mg) in K_2CO_3 buffer (0.1M, pH~9, 6 mL) was mixed with a solution of FITC (0.013 mmol, 5 mg) in acetone (5 mL) and stirred at 4 ºC under nitrogen atmosphere. After 8 h, the precipitate was centrifuged (8000 rpm) and washed with water and MeOH until no free dye was detected in the supernatant solution. The solvent was removed and the solid (**NCP₃-FITC**) was dried under vacuum and characterized. In a second step, 200 μL of an aqueous solution of A568 (0.01 % w/w) and acetic acid (2 μL) were added to a stirring dispersion of **NCP₃-FITC** (5 mg) in 1.2 mL of EtOH. The mixture was stirred under reflux for 6 h. The resulting particles were purified by centrifugation, and then washed with water and EtOH until no free dye was detected in the supernatant solution by UV-Vis. The precipitate (**NCP₃-FITC-A568**) was dried under vacuum overnight and fully characterized. For more information about characterization see Supporting Information, Section S10.

Quantification procedure by HPLC-UV

An HPLC-UV method for the simultaneous quantification of catecholic ligands, bix and fluorescent dyes in NCPs was developed.

Chromatographic conditions: Analyses were performed using a HPLC Waters 2695 separation module coupled to a Waters 2487 UV-Vis detector (suitable for dual detection). The column used was a Chromolith® Performance RP-18e (100 mm x 4.6 mm). Eluent A was a 0.1% (v/v) H_3PO_4 aqueous solution containing 262 mg/L sodium 1-octanesulfonate and eluent B was methanol absolute (HPLC grade). Before the analysis, the RP column was pre-equilibrated using the starting conditions of the method (99 % A (v/v)) for 6 min. The elution began with an isocratic elution of 99% A (v/v) for 5 min, followed by a gradual increase of A from 1% to 40% (v/v) until 25 min. Then, the mobile phase was raised to 98% B (v/v) (between minutes 25 and 30) to elute tight bound compounds and kept at 98% B (v/v) for additional 5 min. Finally, mobile phase was reset to the initial conditions (A:B) 99:1 (v/v) and stayed for 6 min to equilibrate for the next injection. The flow rate was set at 1.0 mL/min and the column temperature was kept at 25 °C. The detection wavelengths were 214 and 280 nm.

Sample preparation: NCPs samples were prepared dissolving 1 mg NCPs/mL in 0.1 mL of a methanol/HCl mixture (50 µL concentrated HCl/mL methanol) containing 20 mg/mL of citric acid. The initial samples were diluted with 0.9 mL of deionized water to have a final water/methanol ratio of 90:10 and sonicated for 5 min. Then, samples were further diluted 4 and 10 times in buffer A before their injection into the HPLC system. All samples were prepared in triplicate.

Calibration curves: A calibration curve using 3,4-dihydroxybenzaldehyde (DHBA), dopamine and 1,4-bis(imidazol-1ylmethyl)benzene (Bix) as external standards was prepared. Standards were prepared by duplicate, diluting a stock solution containing DHBA, dopamine and Bix (522, 440 and 436 µg/mL, respectively) dissolved in a methanol/HCl mixture (50 µL concentrated HCl/mL methanol) and diluted with distilled water to a final water/methanol ratio of 90:10. In both cases, results were adjusted to linear regression models with $R^2 > 0.999$ between the ranges of 9-261, 8-220 and 8-218 µg/mL for DHBA, dopamine and Bix, respectively. Calibration curves for dopamine-FITC and DHBA-PBH were prepared separately by diluting stock solutions of 1.4 and 1.3 mg/mL for dopamine-FITC and DHBA-PBH, respectively. Initial solutions were dissolved in a methanol/HCl mixture (50 µL concentrated HCl / mL methanol) and diluted with distilled water to a final water/methanol ratio of 90:10. An strong linear correlation ($R^2 > 0.97$) was observed between 5-359 and 1-130 µg/mL for dopamine-FITC and DHBA-PBH.

Quantification by UV-Vis analysis

NCP₁-FITC, NCP₂-PBH and NCP₃-FITC-PBH quantification: The quantification of **FITC** and **PBH** in **NCP₁-FITC** and **NCP₂-PBH** was carried out by UV-Vis employing calibration curves (Absorbance vs. Concentration) obtained after preparation of standard solutions with different concentrations of pure dyes in acid medium. For measurements, standard solutions of FITC or PBH in the range of 0.01 – 13 mM were prepared and maximum absorptions were registered at the corresponding wavelength (443 nm for **FITC** and 342 nm for **PBH**). In this way, payload quantification was calculated by measuring the absorbance of the medium after degradation of 1 mg of corresponding NCPn-dye system with strong acid (HCl 36 wt %) and subsequent dilution with water. The absorbance values were interpolated in the corresponding UV-Vis calibration curve and concentration values of dye into NCPn-dye were obtained.

NCP-L₁, NCP-L₂ and NCP-L₁-L₂ quantification: The quantification of **L₁** and **L₂** in **NCP-L₁** and **NCP-L₂** was carried out by UV-Vis employing calibration curves (Absorbance vs. Concentration) obtained after preparation of standard solutions with different concentrations of pure dyes in acid medium. For measurements, standard solutions of **L₁** or **L₂** in the range of 0.01 – 10 mM were prepared and maximum absorptions were registered at the corresponding wavelength (443 nm for **L₁** and 342 nm for **L₂**). In this way, payload quantification was calculated by measuring the absorbance of the medium after degradation of 1 mg of corresponding NCP-Ln system with strong acid (HCl 36 wt %) and subsequent dilution with water. The absorbance values were interpolated in the corresponding UV-Vis calibration curve and concentration values of dye into NCP-Ln were obtained.

In vitro assays

Cell culture: The Human HeLa (ATCC CL-2) cell line was maintained in a Minimum Essential Medium (α-MEM) medium supplemented with 10 % (v/v) of heat inactivated fetal bovine serum (FBS). Cells were grown under a highly humidified atmosphere of 95 % air with 5 % CO_2 at 37 ºC.

In vitro cytotoxicity assay. Cells were seeded in 96-well microassay culture plates at concentration of 2×10^3 cells per well, and grown overnight at 37 °C in a 5% CO_2 incubator. Then, cells were treated with different nanoparticle concentrations (ranging from 1 to 100 µg/ml), or with control medium for 24 h. After incubation, 10 µl of stock ProtoBlue reagent were added to each well. After 2 h at 37 ºC, fluorescence of each well was measured using a microplate reader with an excitation and

emission wavelength of 531 and 572 nm, respectively. Cell cytotoxicity was evaluated in terms of cell-growth inhibition in treated cultures compared to control cells, and expressed as a % of cell viability.

*Cellular uptake of nanoparticle*s: To perform *in vivo* confocal fluorescence microscopy experiments, HeLa cells were seeded in a 35 mm glass-bottom culture dish (MatTek Corporation, Ashland, MA) at a density of 2.0×10^5 cells per dish. After 24 h cells were treated with 50 μg/ml of **NCP₃-FITC-A568,** or with the same concentration of non-functionalized **NCP₃** nanoparticles (as control condition) for 2 h at 37 ºC. Immediately before in vivo imaging, cells were washed twice with 1 ml of fresh Dulbecco´s Modified Eagle Medium (DMEM) medium and then the cell nuclei were stained with Hoechst (Invitrogen) for 10 min. *In vivo* fluorescence imaging was performed in a Leica TCS SP5 confocal fluorescence microscope. Bitplane Imaris software was used for for image processing and data analysis.

In addition to fluorescence microscopy, the intracellular nanoparticle uptake was further evaluated by fluorescence spectroscopy. To perform the experiments, HeLa cells were seeded into six-well plates at a density of 2.0×10^5 cells per well and incubated for 24 h. After incubation, cells were treated with control medium or with **NCP₃-FITC-A568** nanoparticles at two different concentration (50 and 100 μg/mL). After 2 h treatment, the medium was removed, cells were washed twice with PBS and lysed with 1 ml of PBS containing 1% of sodium dodecyl sulphate (SDS). The fluorescence present in all the samples was measured at λ_{em}: 515 and λ_{em}: 583 nm after excitation at λ_{ex}: 470 and λ_{ex}: 568 nm, for the FITC and A568 dyes, respectively. Measurements were performed in a Jasco FP-8200 spectrofluorometer.

Acknowledgements

Keywords: bifunctional nanoparticles • coordination polymers • catechol • fluorescent nanoparticles • functionalization

[1]   J. Della Rocca, D. Liu, W. Lin, *Acc. Chem. Res.* **2011**, *44*, 957–968.

[2]   A. Facchetti, *Angew. Chem., Int. Ed.* **2011**, *50*, 6001–6003.

[3]   W. Lin, W. J. Rieter, K. M. L. Taylor, *Angew. Chem., Int. Ed.* **2009**, *48*, 650–658.

[4]   "Design and Construction of Coordination Polymers" Eds. Mao-Chun Hong, Ling Chen, John Wiley & Sons, 2009, 300 pags.

[5]   C. He, D. Liu, W. Lin, *Chem. Rev.* **2015**, *115* , 11079–11108.

[6]   F. Prins, M. Monrabal-Capilla, E. A. Osorio, E. Coronado, H. S. J. van der Zant, *Adv. Mater.* **2011**, *23*, 1545-1549.

[7]   I. Boldog, A. Gaspar, V. Martínez, P. Pardo-Ibañez, V. Ksenofontov, A. Bhattacharjee, P. Gütlich, J. A. Real, *Angew. Chem., Int. Ed.* **2008**, *47*, 6433-6437.

[8]   a) F. Novio, J. Campo, D. Ruiz-Molina, *Inorg. Chem.* **2014**, *53*, 8742–8748; b) I. A. Gural'skiy, C. M. Quintero, G. Molnár, I. O. Fritsky, L. Salmon, A. Bousseksou, *Chem. Eur. J.* **2012**, *18*, 9946-9954.

[9]   Won Cho, Hee Jung Lee, Sora Choi, Yoona Kim, Moonhyun Oh, *Sci Rep.* **2014**; 4: 6518.

[10]   Z. Qi, Q. You, Y. Chen, *Anal. Chim. Acta* **2016**, *902*, 168–173.

[11]   X. Songab, Y. Maab, X. Geab, H. Zhoua, G. Wanga, H. Zhanga, X. Tangc, Y. Zhang, *RSC Adv.* **2017**, *7*, 8661-8669.

[12]   L. E. Kreno, K. Leong, O. K. Farha, M. Allendorf, R. P. Van Duyne, J. T. Hupp, *Chem. Rev.* **2012**, *112*, 1105−1125.

[13]   F. Novio, D. Ruiz-Molina, *RSC Adv.* **2014**, *4*, 15293-15296.

[14]   Z.-R. Jiang, J. Ge, Y.-X. Zhou, Z. U. Wang, D. Chen, S.-H. Yu, H-L Jiang, *NPG Asia Materials* **2016**, *8*, e253.

[15]   a) F. Novio, J. Simmchen, N. Vázquez-Mera, L. Amorín-Ferré, D. Ruiz-Molina, *Coord. Chem. Rev.* **2013**, *257*, 2839–2847; b) M. Borges, S. Yu, A. Laromaine, A. Roig, S. Suárez-García, J. Lorenzo, D. Ruiz-Molina, F. Novio, *RSC Adv.* **2015**, *5*, 86779–86783.

[16]   F. Novio, J. Lorenzo, F. Nador, K. Wnuk, D. Ruiz-Molina, *Chem. Eur. J.* **2014**, *20*, 15443–15450.

[17]   P. González-Monje, F. Novio, D. Ruiz-Molina, *Chem. Eur. J.* **2015**, *21*, 1−7.

[18]   O. S. Wolfbeis, *Chem. Soc. Rev.,* **2015**, *44*, 4743—4768.

[19]   M. Sun, B. Sun, Y. Liu, Q.-D. Shen, S. Jiang, *Sci. Rep.* **2016**, 6:22368.

[20]   a) E. S. O'Neill, J. L. Kolanowski, G. H. Yin, K. M. Broadhouse, S. M. Grieve, A. K. Renfrew, P. D. Bonnitcha, E. J. New, *RSC Adv.* **2016**, *6*, 30021-30027; b) S. J. Dorazio, A. O. Olatunde, J. A. Spernyak, J. R. Morrow, *Chem. Commun.* **2013**, *49*, 10025-10027.

[21]   F. Nador, K. Wnuk, C. Roscini, R. Solorzano, J. Faraudo, D. Ruiz-Molina, F. Novio, *submitted*

[22]   A. B. Lopes, E. Miguez, A. E. Kümmerle, V. M. Rumjanek, C. A. Manssour Fraga, E. J. Barreiro, *Molecules* **2013**, *18*, 11683-11704.

[23]   F. M. Winnik, *Chem. Rev.* **1993**, *93*, 587–614.

[24]   a) Q. Li, Y. Kim, J. Namm, A. Kulkarni, G. R. Rosania, Y.-H. Ahn, Y.-T. Chang, *Chem. Biol.* **2006**, *13*, 615–623; b) G. R. Rosania, J. W. Lee, L. Ding, H. S. Yoon, Y. T. Chang, *J. Am. Chem. Soc.* **2003**, *125*, 1130–1131.

[25]   S. N. Tammam, H. M. Azzazy, H. G. Breitinger, A. Lamprecht, *Mol. Pharmaceutics* **2015**, *12*, 4277–4289

[26]   C. W. Pouton, K. M. Wagstaff, D. M. Roth, G. W. Moseley, D. A. Jans Adv. Drug Deliv. Rev. **2007**, *59*, 698-717.

Entry for the Table of Contents (Please choose one layout)
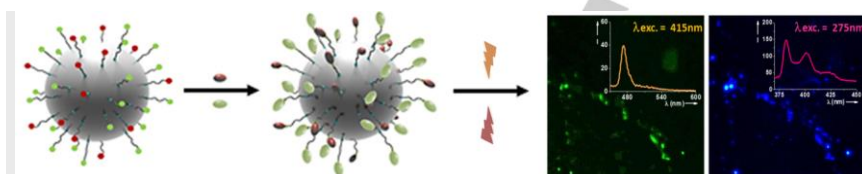
Layout 1:

FULL PAPER

Text for Table of Contents

((Insert TOC Graphic here: max. width: 5.5 cm; max. height: 5.0 cm))
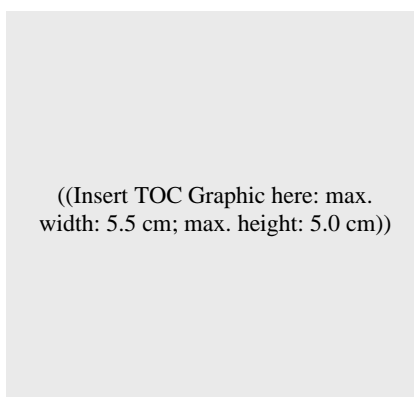
Author(s), Corresponding Author(s)*

Page No. – Page No.

Title

Layout 2:

FULL PAPER

Dr. Fabiana Nador,* Karolina Wnuk, Dr. Javier Garcia-Pardo, Dr. Julia Lorenzo, Rubén Solorzano, Dr. Daniel Ruiz-Molina, and Dr. Fernando Novio*

Dual-fluorescent imaging probes: A series of dual-fluorescent nanoscale coordination polymers with potential use in bioimaging has been prepared via a mixed-ligand synthetic strategy using two approximations: a) a two-step protocol where mixed-ligand nanoparticles were post-functionalized with different dyes, and b) a one-step synthesis where the nanoparticles were formed using pre-functionalized ligands. In vitro studies were performed in order to stablish the viability of the resulting materials.

Page No. – Page No.

Dual-fluorescent nanoscale coordination polymers via a mixed-ligand synthetic strategy and their use for multichannel imaging